Volume 2 Issue 2 (September 2022)
DOI 10.24191/jaeds.v2i2.47
eISSN 2805-5756

Journal of Applied Engineering Design & Simulation

Finite Element Analysis for Rocket Motor Case Under Internal Pressure and Thermal Loads

M. A. Muhammad[1,2], Z. Salleh[1*], A. H. A. Hamid[1], M. J. Sujana[2] and K. Kamaludin[2]
[1]High Energy Material Research Laboratory (HEMREL), School of Mechanical Engineering, College of Engineering, Universiti Teknologi MARA, Shah Alam 40450 Selangor, Malaysia
[2]MTC Defence, MTC Engineering Sdn. Bhd., 2 Jalan Astaka U8/88B, Seksyen U8 Bukit Jelutong, 40150 Shah Alam, Selangor, Malaysia
*Corresponding author: szuraidah@uitm.edu.my

ABSTRACT

Rocket motor combustion chamber needs to contain very high pressure and temperature due to burning of rocket fuels. For that reason, the combustion chamber is required to withstand the stresses caused by the static and thermal load generated by the burning of the rocket fuels. History demonstrated that a strong rocket motor case can fail due to thermal load neglection. In this study, it has been proven that thermal load affects the stresses produced on the rocket motor case. The stresses produced by the internal pressure and thermal load are called overall stresses. In this study, the thermal analysis was done using ANSYS software with various thickness of CC 2.5, CC 3.5 and C.C 5.0 in two conditions which were the stress due to static stress and the stress due to static and thermal loads. The propellant properties, pressure applied, chamber temperature and heat coefficient were the same in all cases. The maximum von-Mises stress for static load increased from lower to higher thickness with 69.35 MPa, 51.78 MPa and 34.8 MPa for CC 2.5, CC 3.5 and CC 5.0, respectively. When the thermal load was applied, the maximum von-Mises stress increased from 51.78 MPa to 76.87 MPa for CC 3.5, and from 34.80 MPa to 42.61 MPa for CC 5.0. The trend for overall stresses also increased from 68.56 MPa for CC 2.5 to 76.88 MPa for CC 3.5. This study shows that when a thermal load is applied to the rocket body case, the maximum von-Mises stress will also increase.

Keywords: stress analysis, rocket motor, combustion chamber, hoop stress, ANSYS

Nomenclature

h	Convective heat transfer coefficient (W/(m^2.K))
c^*	Characteristic velocity (m/s)

Abbreviations

2D	Two Dimensional
ANSYS	Analysis System
AP	Ammonium Perchlorate
CC	Combustion Chamber
AL	Aluminum
HTPB	Hydroxyl-terminated Polybutadiene
MET	Malaysia Meteorological Department
NADMA	National Disaster Management Agency
ProPeP	Propellant Evaluation Program
RMAF	Royal Military Air Force
SPEI	Standardized Precipitation Evapotranspiration Index
SPI	Standardized Precipitation Index

Received on 07.03.2022
Accepted on 03.08.2022
Published on 23.09.2022

1.0 INTRODUCTION

Universiti Teknologi MARA (UiTM) and MTC Engineering Sdn. Bhd. have a strategic research partnership between university and industry. This research partnership develops a cloud-seeding rocket that can achieve functional results within a low budget constraint and short time frame. The project is planned to easily use the available raw materials for the propellant such as potassium nitrate oxidizer and sugar-based fuels. This will lower the budget and shorten the time frame for the project compared to the use of commonly high specific impulse rocket fuel materials such as ammonium perchlorate, potassium perchlorate and hydroxyl terminated polybutadiene (HTPB) due to the restricted import law [1].

Climate change occurs all around the world and it affects Malaysia too. One of the climate changes that affect Malaysia is drought which causes progressive increasing temperature in the future [2]. The significance of temperature for the drought formation is measured by Standardized Precipitation Index (SPI) and Standardized Precipitation Evapotranspiration Index (SPEI). Study showed that the SPI and the SPEI are greatly affected by the short-term (1-month) rainfall where less rainfall in a month will cause less SPI [2]. Extreme and dry seasons cause prolonged droughts that affect the vegetation health and threaten national food security. Therefore, cloud-seeding is an alternative developed to mitigate low precipitation rate during dry seasons by artificially improving cloud's ability to produce rainfall.

Generally, cloud seeding is done by two methods, aerial and ground based. Aerial cloud seeding is more favorable as it is more effective and usually uses smaller aircrafts. However, it is costly and dangerous to seed cloud using small aircrafts [3]. Currently in Malaysia, the Meteorological Department (MET) uses two types of aircrafts for aerial methods. One of them is using Cessna 172 that carries cloud seeding flares up to 300 feet (915 meter) and burns the flare by releasing sodium chloride and magnesium oxide on the updraught under the targeted potential clouds, in which this operation is under the authorization of MET and operated by AFJets Sdn. Bhd [4]. An alternative method done by MET with the collaboration of National Disaster Management Agency (NADMA) and Royal Military Air Force (RMAF) is by carrying mixed of salt solution and water, and this solution is sprayed to the targeted cloud to enhance the formation of rain droplets [5].

The other aerial-based method is cloud seeding rocket. Cloud seeding using rocket has become common in countries such as China, since they have been known for firing cloud seeding rockets in 2008 during the Beijing Olympic to make sure the event is rain free [6]. The rockets carry chemical composition in the form of flare in the payload section. The chemical compositions consist of particles like silver iodine which essentially acts as nuclei for raindrops to form, allowing water droplets to coalesce until they become so heavy that they fall from the sky as rain or snow [7].

There have been many components of rocket being studied, and the basic ones include nose cone, rocket body, fins and rocket engine or motor. There are many sub-components for rocket motor, but this study focuses on rocket motor casing. Nose cone design will affect the drag force experienced by the rocket, and common study has shown that the shapes with the best aerodynamics demonstrated are elliptical shape and tangent shape, with parabolic shape in third place [8]. While the function of the fins is to make sure the rocket can fly dynamically stable as it widens the surface area and lowering the centre of pressure, the design of the fins must be optimized to provide sufficient stability and minimize drag [9].

Thermal stress is concerned with imported body temperature as the load to the structure. When pressure is also applied, a combination of thermal stress and static stress is known as overall stress. Therefore, the motor case and thermal analysis come together as they are very closely related to the success of this project. In this study, the casing was made from Molybdenum because it exhibits large mechanical resistance when operated at high temperatures. Analysis was done using ANSYS, a commercially available software used to determine the suitability of the material as a rocket motor casing. Thus, the objective of this study is to analyse the structural and thermal effects of combustion in the solid rocket motor casing with varying thickness.

2.0 METHODOLOGY

Initially, the properties of Molybdenum are recorded into the Engineering Data of ANSYS Workbench software based on Table 1.

Table 1. The list of Molybdenum Properties in Analysis System (ANSYS) software [10]

Material	Molybdenum
Density (g/cm^3)	10.24
Thermal Conductivity, k (W/m.K)	142
Yield Strength (MPa)	110
Coefficient of Thermal Expansion (1/K)	5.2×10^{-6} at 293.15K
Young's Modulus (MPa)	3.2×10^5
Specific Heat (J/kg.K)	251
Poisson's Ratio	0.32
Emissivity	0.64 on outer wall & 0.038 on inner wall

2.1 Propellant parameters

The heat exchange coefficient for propellant was calculated as shown below in Equation (1) whereas the Chamber Temperature was obtained from Propellant Evaluation Program (ProPeP) software for AP/AL/HTPB solid propellant. ProPeP is a thermochemical software that allows the user to evaluate the theoretical performance of a solid (or liquid) rocket propellant. It is particularly useful for checking the viability of possible propellant formulations. It also allows the user to quickly determine the most effective ratios of ingredients to achieve the desired performance, from a theoretical perspective.

$$h = C\frac{C_p G^{0.8}}{D_i^{0.2}}\left[1+\left(\frac{D_i}{L}\right)^{0.7}\right] \quad (\mathrm{W/(m^2K)}) \qquad (1)$$

where h is the convective heat transfer coefficient. The properties of AP/AL/HTPB are shown in Table 2.

Table 2. Propellant Properties of AP/AL/HTPB [11]

Type of Propellant	Solid
Composition of AP/AL/HTPB	68: 17: 15
Inner Pressure (MPa)	6.895
Mass of AP/AL/HTPB/IPDI (g)	204: 45: 51: 6.63
Convective heat coefficient (W/m^2K)	302.17
Chamber Temperature (K)	2854.64
Characteristic Velocity* (m/s)	1548.08
Average molar mass (g/mol)	25.14
Average Cp (kJ/kg.K)	1.203
Mass flow rate (kg/s)	0.10221
Specific Impulse (s)	192.643
Burn time (s)	3

2.2 Combustion chamber

CC acts as a housing for igniter, propellant, copper wire and nozzle. Assumptions of thick-walled cylinder include that the cylinder is made up of isotropic and homogeneous material, longitudinal stresses are uniform across the thickness of the wall and the cylinder experiences uniform internal pressure. Figure 1 illustrates CC with its components [12].

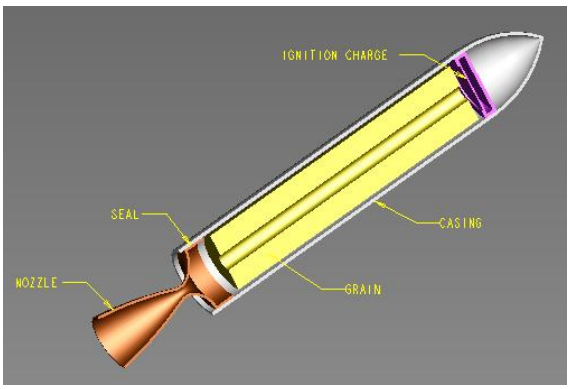

Figure 1. Rocket motor components[12]

The CC was designed in the Design Modeler with thickness of 5mm and length of 100mm which was converted into ANSYS mechanical with 2D Axisymmetric of 10° angle to show half view of hollow cylinder. Element size of 1mm was chosen for meshing.

Static structural analysis was conducted with one end clamped and pressure load of 6.895MPa on the inner wall of the casing. This is to obtain radial, hoop and Von Mises Stress. Then, steady thermal analysis has boundary conditions of radiation and convection as in Table 1 and Table 2. This analysis is to compute the temperature distribution and heat flux. Thermo-structural analysis was then performed with applied thermal and structural load from the previous two analyses. This helps to compute the overall hoop, radial and Von Mises stress to obtain the safety factor of the rocket motor casing.

3.0 RESULTS AND DISCUSSION

3.1 Overall stress analysis

Thermal stress is concerned with the imported body temperature as the load to the structure. When pressure is also applied, a combination of thermal stress and static stress is known as overall stress [13].

3.1.1 Overall radial stress of CC 2.5, CC 3.5 and CC 5.0

Overall radial stress basically uses the same concept as radial stress but with the condition of temperature involved. Radial stress is generally much smaller in terms of magnitude of stress as compared to hoop stress [14]. The readings of overall radial stress should be higher than in radial stress as temperature is also taken into account with pressure of 6.895MPa. Figure 2, Figure 3 and Figure 4 show the visual representation of overall radial stress throughout its thickness. Figure 5 shows the comparison of the three models in graphical form.

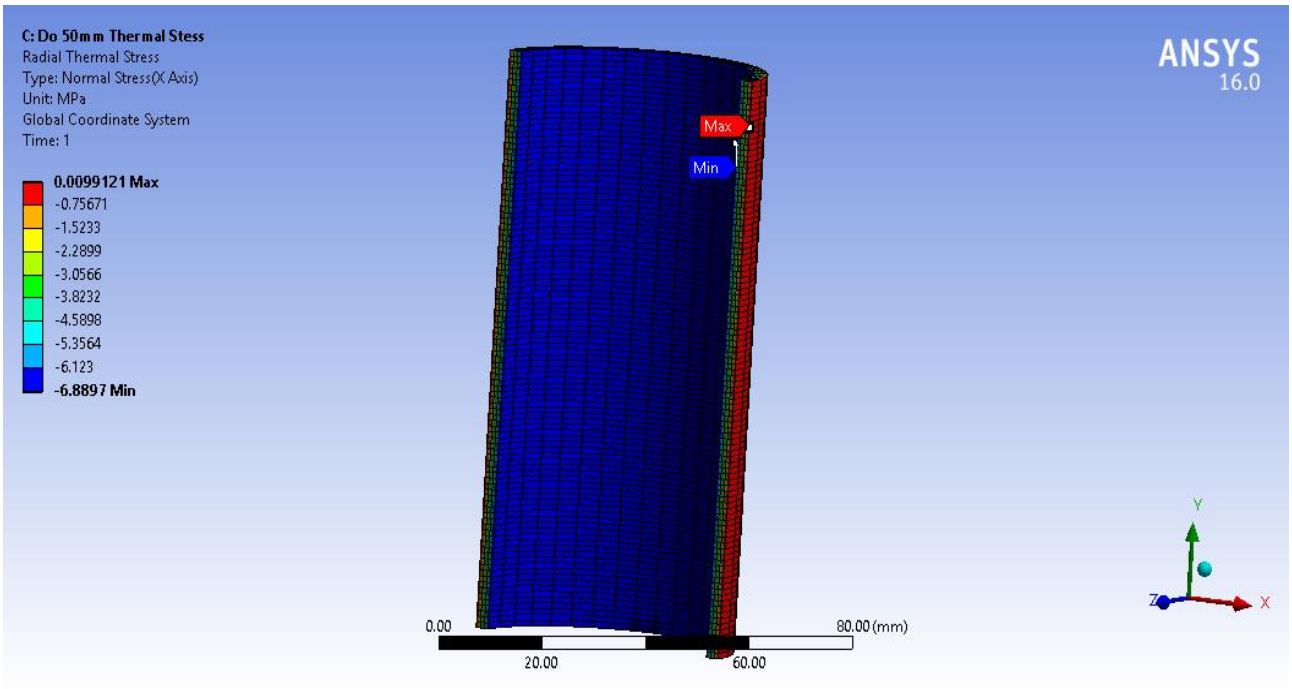

Figure 2. Overall radial stress of CC 2.5

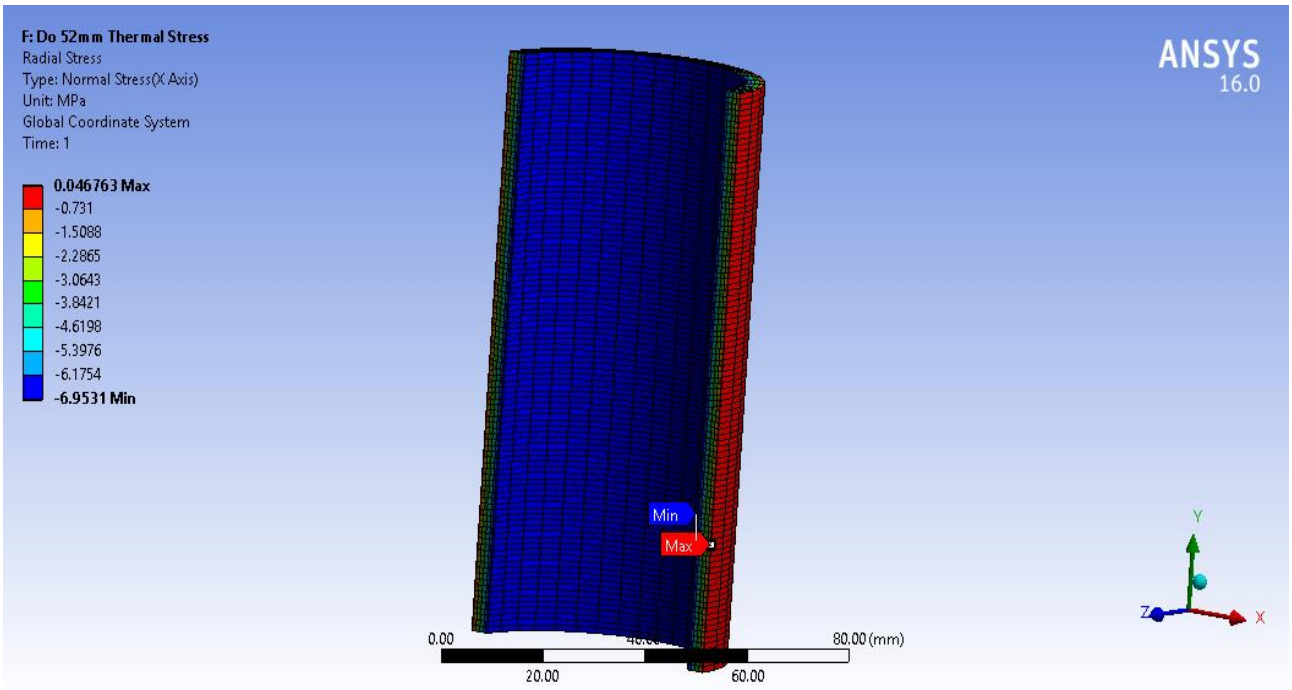

Figure 3. Overall radial stress of CC 3.5

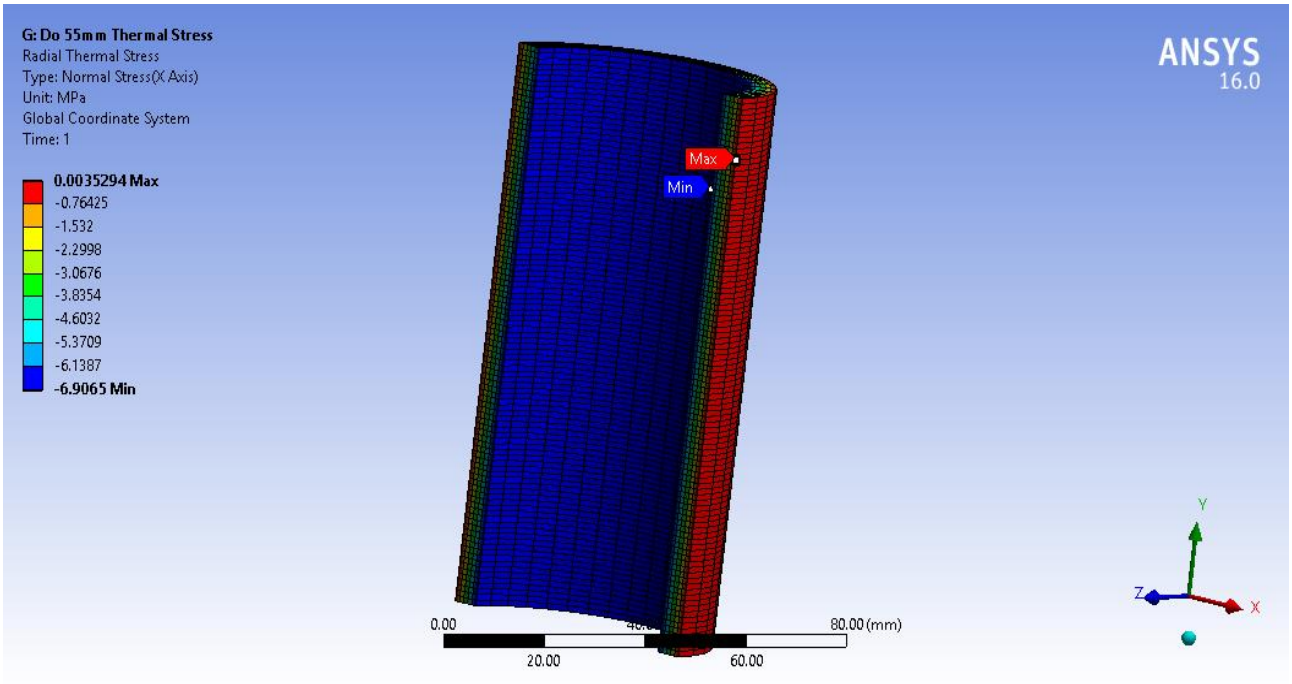

Figure 4. Overall Radial Stress of CC 5.0

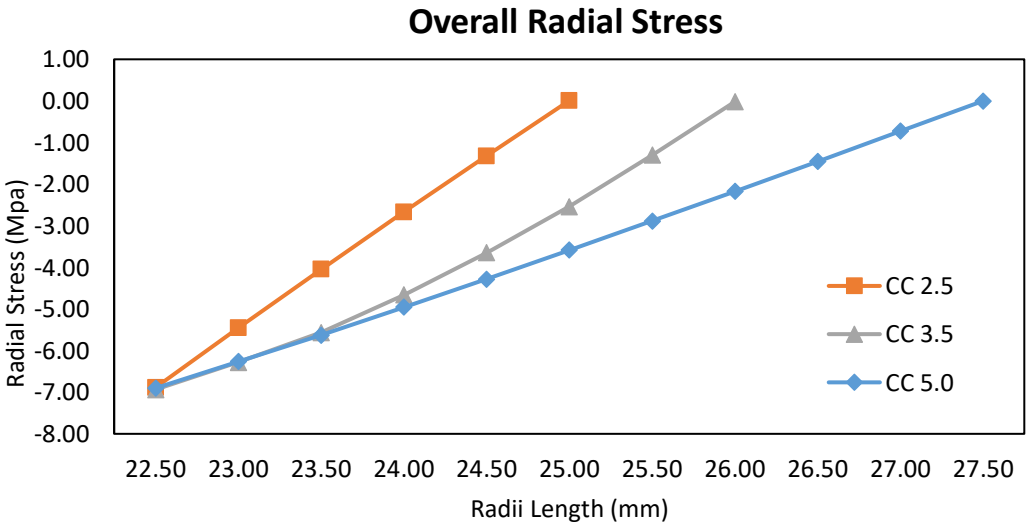

Figure 5. Overall radial stress of CC 2.5, CC 3.5 and CC 5.0

There is a steeper increase in overall radial stress for CC 2.5. The maximum value of overall radial stress is -6.8874MPa which increases to a minimum value of 0.0064MPa. Contrasting this with the green line, CC 3.5 with outer diameter of 52mm, the trend of the graph shows that it curves slightly upwards. This is due to the changes in temperature and heat flux per unit area based on the thermal analysis simulation. The maximum value of overall radial stress is -6.9365MPa which is the highest amongst the three models. This means that CC 3.5 has the highest compression through the stress across the x-axis of the model.

CC 5.0 has a maximum overall radial stress of -6.9021MPa which is lower than CC 3.5 but higher than CC 2.5 in terms of compression. A linear increase of overall radial stress reaches the minimum value of -0.0016MPa for this simulation result.

This would mean that radial stress increases linearly when subjected to thermal and structural loadings [15]. As the thickness of the radius of the casing increases, the values of radial stress are more stretched out; hence, it shows no significant deformation on the structure [16]. In accordance with Lamé's Theory, radial stress is the highest in compression at the inner wall of the casing [17].

3.1.2 Overall hoop stress of CC 2.5, CC 3.5 and CC 5.0

Overall hoop stress, however, is much higher than the overall radial stress values. Overall hoop stress is concerned with the application of pressure and temperature towards the circumferential stress [14]. Figure 6, Figure 7 and Figure 8 show the visual representation of overall hoop stress throughout its thickness. Figure 9 shows the comparison of the three models in graphical form. Hoop stress is inversely proportional to the thickness of the cylinder. Supposedly, the maximum value is evident for the smallest thickness of cylinder.

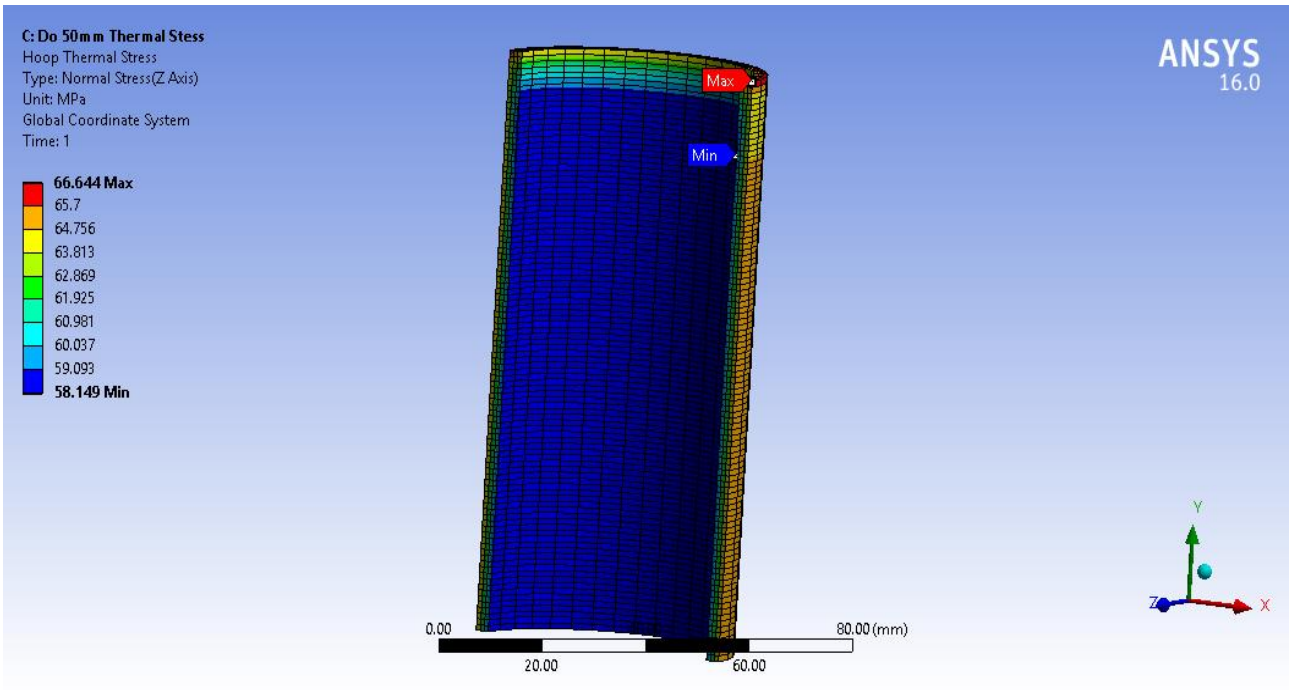

Figure 6. Overall Hoop Stress of CC 2.5

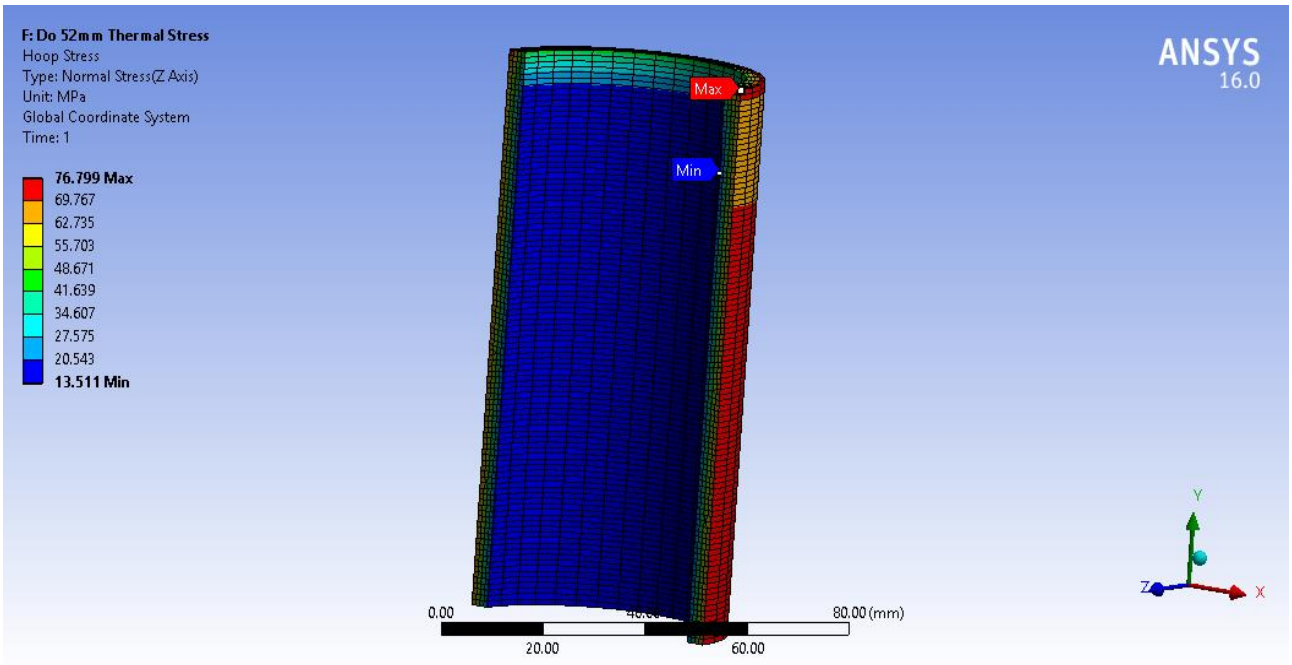

Figure 7. Overall Hoop Stress of CC 3.5

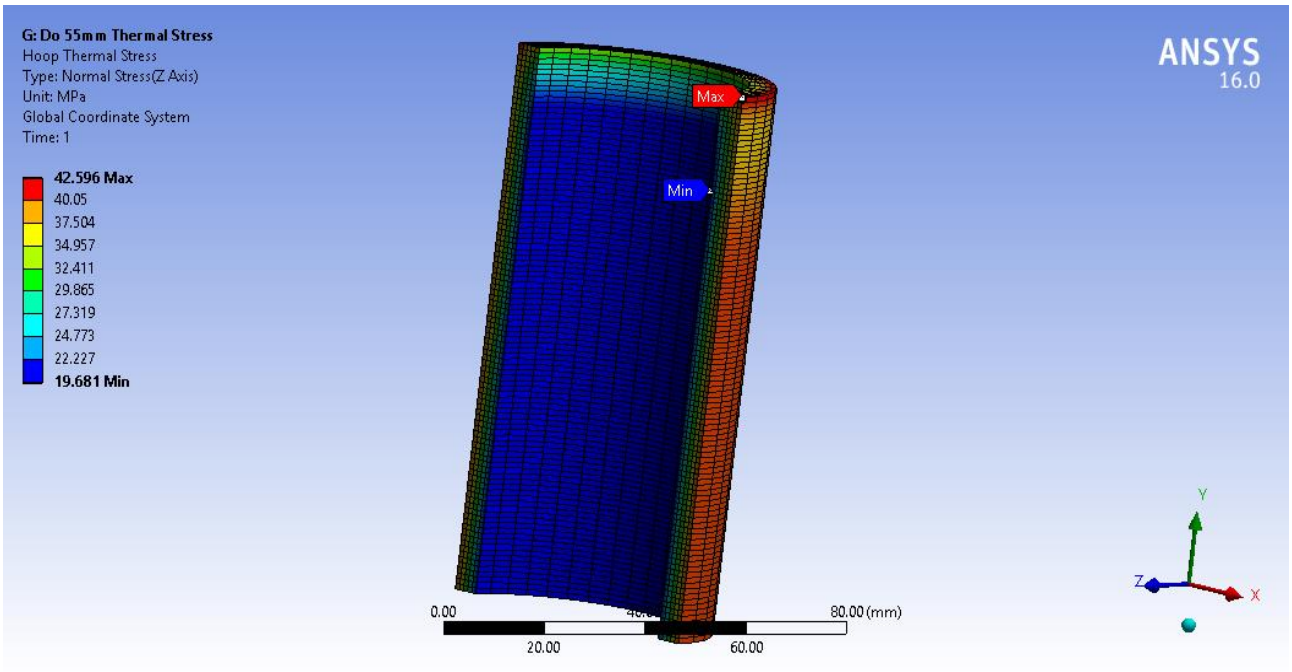

Figure 8. Overall Hoop Stress of CC 5.0

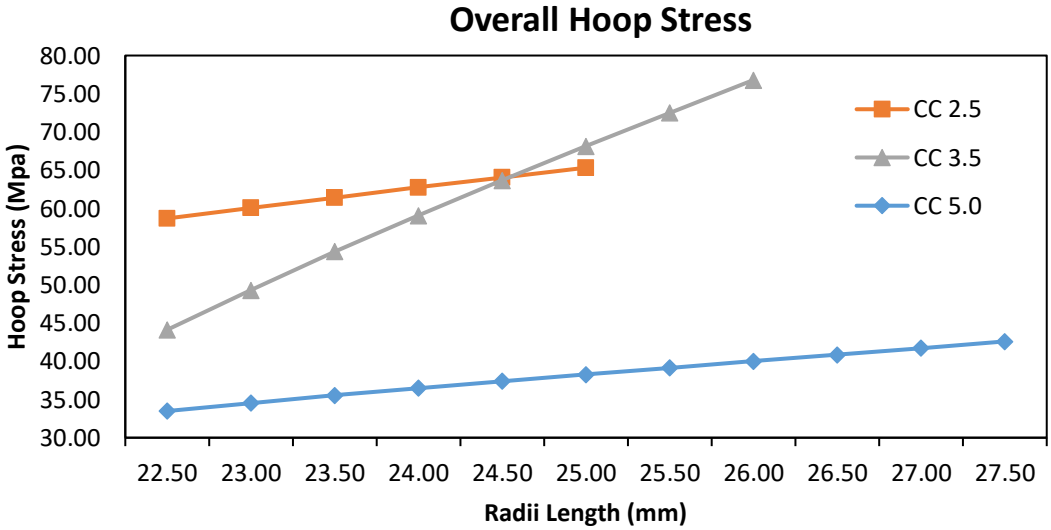

Figure 9. Overall Hoop Stress of CC 2.5, CC 3.5 and CC 5.0

Hoop stress is inversely proportional to the thickness of the cylinder. Supposedly, the maximum value is evident for the smallest thickness of cylinder [17]. All three models show an increase in overall hoop stress across thickness of the casings. The initial values of overall hoop stress are 58.686MPa, 44.1180MPa and 33.4870MPa for CC 2.5, CC 3.5 and CC 5.0. Overall hoop stress is inversely proportional to the thickness of the casing. This is observed as increasing thickness of the casing results in lower values of hoop stress. However, CC 3.5 exhibits a different behaviour in which the maximum value of overall hoop stress exceeds other models. This is due to the combined effect of large temperature gradient of 17.9K and large pressure applied on the inner wall of the casing.

Therefore, the highest value of overall hoop stress occurs on the green line, the model with an outer diameter of 52mm at 76.7990MPa. This is much higher than the values of 65.3240MPa and 42.5960MPa for models with outer diameter of 50mm and 55mm. Lamé's Theory states that hoop stress has a maximum value on the outer wall of the casing [18]. This is in accordance with the thickness of the casing. However, CC 3.5 exhibits a different behaviour in which its maximum value is the highest amongst the three models. This would mean that when temperature is an applied boundary condition, the values of overall hoop stress would increase significantly depending on the large temperature gradient of the casing [19].

3.1.3 Overall Von Mises Stress of CC 2.5, CC 3.5 and CC 5.0

Overall Von Mises stress or equivalent stress takes into account all stresses and thermal conditions acting on the casing [15]. This means that overall radial and hoop stress are taken into account along with imported body temperature of thermal analysis to compute the overall stress values for the three models [19]. Figure 10, Figure 11 and Figure 12 show the visual representation of overall von mises stress throughout its thickness. Figure 13 shows the comparison of the three models in graphical form. Since the overall radial stress is small in comparison to the overall hoop stress, Figure 13 shows a similar upward trend of thermal stress as in the overall hoop stress. The values of overall von mises stress are evidently higher than that of overall hoop stress. This is because von mises stress takes into account all stress acting upon it and is therefore much higher than the values of other stresses in a singular direction.

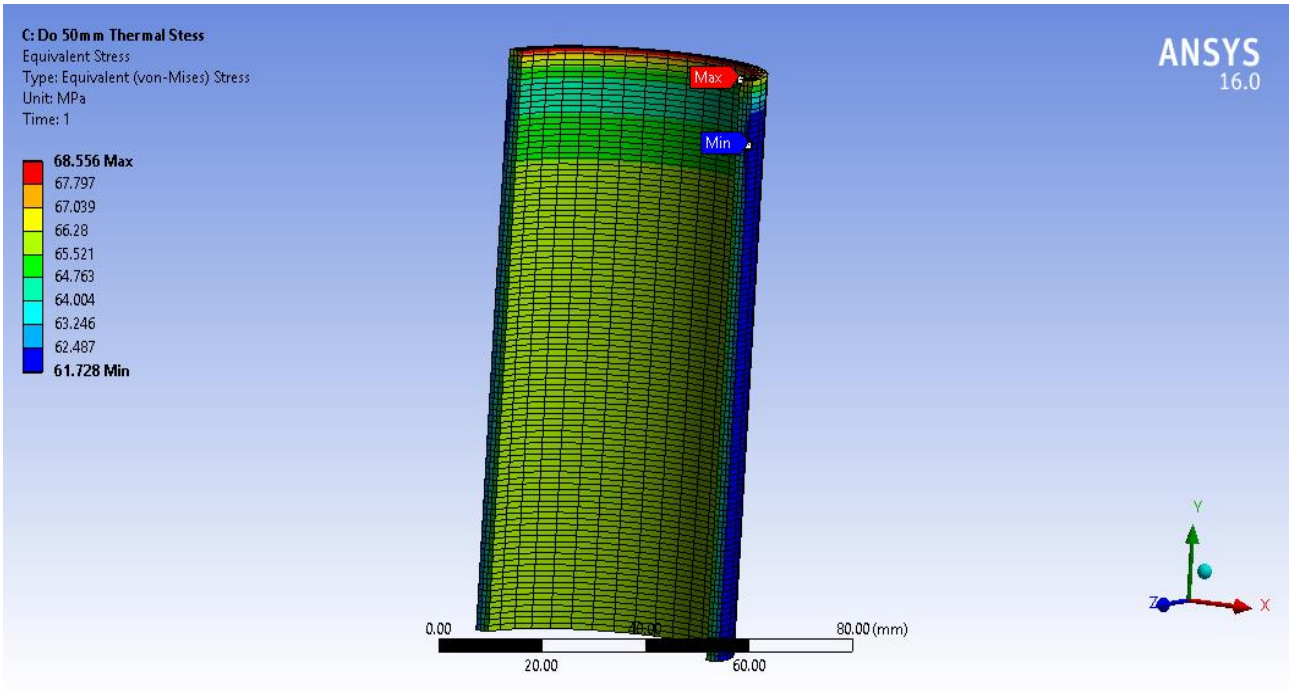

Figure 10. Overall Von Mises Stress of CC 2.5

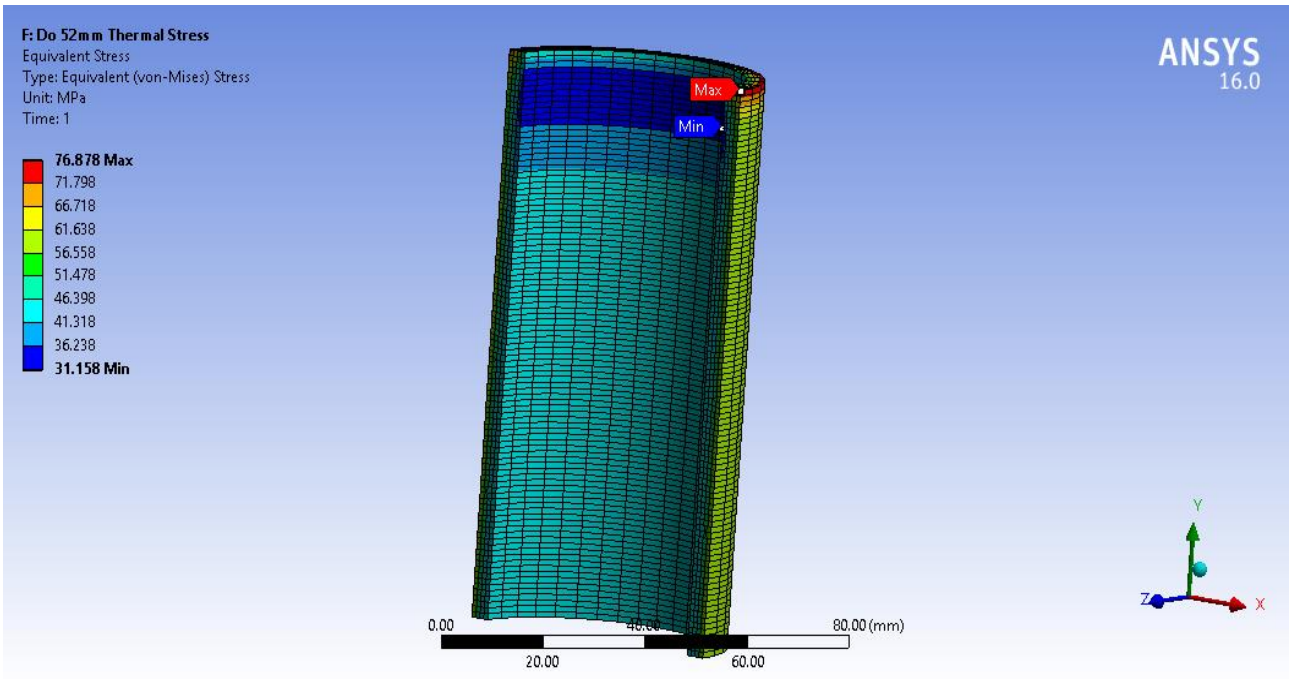

Figure 11. Overall Von Mises Stress of CC 3.5

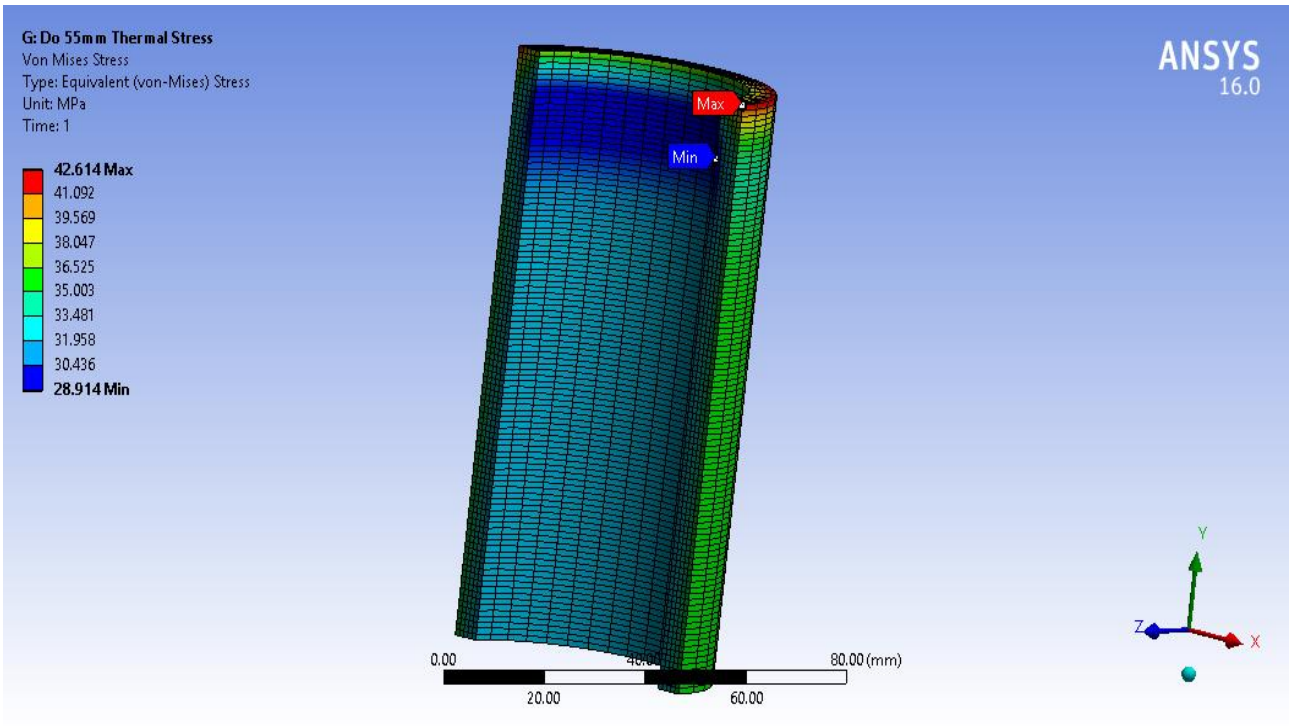

Figure 12. Overall Von Mises Stress of CC 5.0

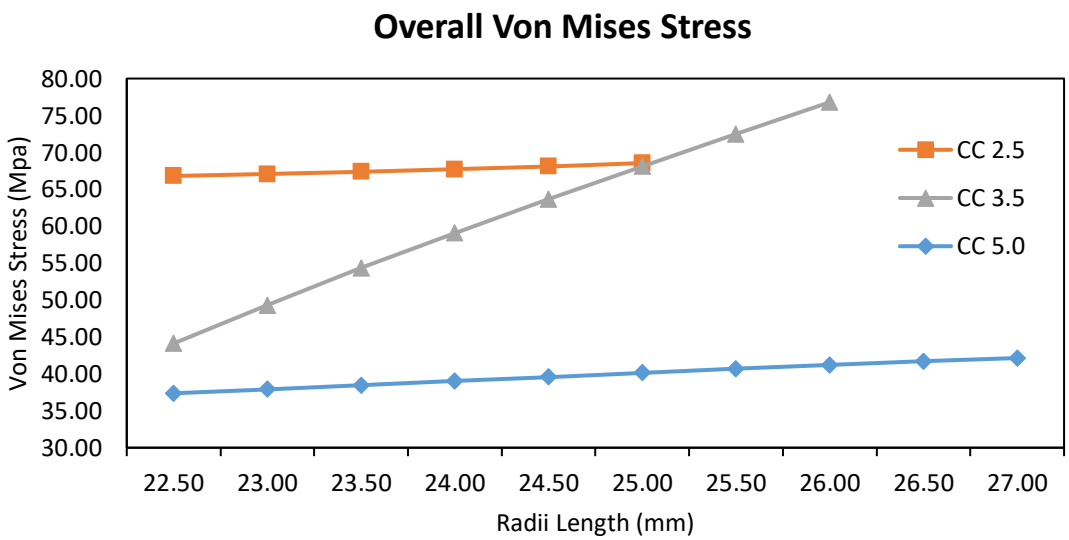

Figure 13. Overall Von Mises Stress of CC 2.5, CC 3.5 and CC 5.0

For an outer diameter of 50mm, CC 2.5 has an overall von mises stress increase of 66.8010MPa to 68.5560MPa from the inner wall to the outer wall of the casing. This shows a small overall stress difference of 1.755MPa. Then, the model with an outer diameter of 52mm, CC 3.5 has an overall von mises stress increase of 47.8480MPa to 76.8780MPa from the inner wall to the outer wall of the casing. This shows the largest stress difference of 29.03MPa.

Lastly, for an outer diameter of 55mm, CC 5.0 has the equivalent stress increasing gradually from 37.3740MPa to 42.6140MPa. The stress difference is about 5.24MPa for the casing with a thickness of 5mm. CC 5.0 and CC 2.5 experience a small gradual increase in terms of overall von mises stress but CC 3.5 has a steep increase. The large temperature gradient experienced by CC 3.5 is the cause of the steep change in stress for both overall hoop stress and overall von mises stress.

Therefore, thermal stress is inaccurate to be used to compute the total stress of the structure. A combined thermo-structural analysis is necessary to obtain the overall stress values. Theoretically, as the thickness of the casing increases, the radial, hoop and von mises stresses increase accordingly. CC 3.5 experiences a large temperature gradient and therefore bested the other two models in terms of overall hoop and von mises stress.

The safety factor was also computed in Table 3 for CC 2.5, CC 3.5 and CC 5.0 at 1.6045, 1.4308 and 2.5813 respectively with reference to the yield strength of Molybdenum. CC 3.5, therefore, has the smallest safety factor followed by CC 2.5 and CC 5.0. Theoretically, CC 5.0 has the highest safety factor which should be the best choice.

Table 3. Safety Factor of CC 2.5, CC 3.5 and CC 5.0

Size	CC 2.5	CC 3.5	CC 5.0
Safety Factor	1.6045	1.4308	2.5813

3.2 Complete overview

CC 2.5 shows that radial, hoop and von mises stresses are significantly larger in compression than CC 3.5 and CC 5.0 when a pressure of 6.895MPa is applied. Negative values of stress represent compression whereas positive values indicate result of tension. However, the final temperature for CC 2.5 is the highest amongst the three models at 1690.5K. The temperature distribution shows that there is a larger slope for CC 3.5 and it has the largest temperature drop amongst the three models. Temperature is still lowest on the inner and outer wall of the cylinder when evaluated on CC 5.0. The heat flux, however, almost coincides for CC 2.5 and CC 3.5. This means that there is similar heat transfer rate for the two models but it is the highest at an outer diameter of 55mm in CC 5.0.

Overall radial stress is almost similar to the trend of radial stress due to the application of high pressure on the inner wall of the casing. CC 3.5, however, coincides with CC 5.0 in radial stress as it stays in compression slightly longer than CC 2.5. The overall hoop stress for CC 3.5 reaches an ultimate high of 76.799MPa which is higher than that in CC 2.5 and CC 5.0 due to the large temperature gradient in static thermal analysis. The overall von mises stress is also similar to overall hoop stress as it is the total stress acting on the casing. CC 5.0 shows a steady increase in overall radial, hoop and von mises stresses. This also means that the amount of stress increases slowly with the radii length. The highest slope is evident in CC 2.5 for overall radial, hoop and von mises stresses. This means that there is a faster change in overall stress across to the thickness of the casing.

Table 4. Overall Results

Model	CC 2.5	CC 3.5	CC 5.0
Outer Diameter (mm)	50	52	55
Thickness (mm)	2.5	3.5	5.0
Volume (mm3)	37311.25	53335.45	78550.00
Nodes	1107	1399	1711
Element	300	398	500
Maximum Radial Stress (MPa)	-6.8715	-6.8753	-6.8757
Maximum Hoop Stress (MPa)	65.6600	48.0020	34.8000
Maximum Von Mises Stress (MPa)	69.3520	51.7830	38.6990
Final Temperature (K)	1690.50	1675.20	1660.90
Maximum Heat Flux (W/m2K)	0.3312	0.3322	0.3394
Maximum Overall Radial Stress (MPa)	-6.8874	-6.9365	-6.9021
Maximum Overall Hoop Stress (MPa)	65.3240	76.7990	42.5960
Maximum Overall Von Mises Stress (MPa)	68.5560	76.8780	42.6140
Safety Factor	1.6045	1.4308	2.5813

CC 2.5 results in a safety factor of 1.6045. Hence, the safety factor of CC 3.5 is the lowest at 1.4308. The safety factor for CC 5.0 is therefore the highest at 2.5813. CC 3.5 is undesirable as it has the lowest safety factor. CC 2.5 is a better choice than CC 5.0 as weight plays an important role in smaller sized rockets. This is observed as CC 2.5 has the lowest volume of the solid rocket motor casing.

4.0 CONCLUSIONS

The overall stress analysis was done on the rocket motor casing with three different wall thickness. The maximum von-Mises stress for static load increases from lower to higher thickness which are 69.35 MPa, 51.78 MPa and 34.8 MPa for CC 2.5, CC 3.5 and CC 5.0, respectively. When the thermal load is applied, the maximum von-Mises stress increases from 51.78 MPa to 76.87 MPa for CC 3.5, and from 34.80 MPa to 42.61 MPa for CC 5.0. The trend for overall stress also increases from 68.56 MPa for CC 2.5 to 76.88 MPa for CC 3.5. This study shows that when a thermal load is applied to the rocket body case, the maximum von-Mises stress will also increase. It is recommended to study the significance of weight due to higher thickness to the performance of the rocket since it is true that greater wall thickness has higher safety factor when applied to static and thermal load.

ACKNOWLEDGMENT

This publication was supported by the Strategic Research Partnership grants 100-RMC 5/3/SRP PRI (024/2020) and 100-RMC 5/3/SRP (020/2020), and Micro-Industry Hub (MIH) Program (MIH-(005/2020)), a funded program under Universiti Teknologi MARA and MTC Engineering Sdn Bhd.

REFERENCES

[1] James C. Thomas, Gordon R. Morrow, Catherine A.M. Diller, and Eric L. Peterson, "Comprehensive study of ammonium perchlorate particle size/concentration effects on propellant combustion," in *Journal of Propulsion and Power*, 2020, vol. 36, no. 1, pp. 95–100. doi: 10.2514/1.B37485.

[2] K. F. Fung, Y. F. Huang, and C. H. Koo, "Assessing drought conditions through temporal pattern, spatial characteristic and operational accuracy indicated by SPI and SPEI: Case analysis for Peninsular Malaysia," *Natural Hazards*, vol. 103, no. 2, pp. 2071–2101, Sep. 2020, doi: 10.1007/s11069-020-04072-y.

[3] H. A. Israr, "An Overview of Using Unmanned Aerial Vehicle as an Alternative Solution for Cloud Seeding Process," Johor, Jan. 2016. [Online]. Available: www.jtse.utm.my

[4] Reuters Staff, "Smothered by smoke, Malaysia seeds clouds to bring rain relief | Reuters," *Reuters*, Sep. 18, 2019. https://www.reuters.com/article/us-southeastasia-haze-idUSKBN1W31CG (accessed Apr. 18, 2022).

[5] Mymilitarytimes Staff, "RMAF Carries Out Cloud Seeding in Kedah and Perlis - MY Military Times," *mymilitarytimes*, Feb. 15, 2020. https://mymilitarytimes.com/index.php/2020/02/15/rmaf-carries-out-cloud-seeding-in-kedah-and-perlis/ (accessed Apr. 18, 2022).

[6] News18 Staff, "How Dubai Created Artificial Rain With Cloud Seeding," *News18.com*, Jul. 24, 2021. https://www.news18.com/news/buzz/read-how-dubai-created-fake-rain-with-cloud-seeding-3999557.html (accessed Apr. 17, 2022).

[7] Mack DeGeurin, "China Used Rockets to Control Weather for Communist Party Event," *Gizmodo*, Aug. 12, 2021. https://gizmodo.com/china-is-using-rockets-to-control-the-weather-1848175761 (accessed Apr. 17, 2022).

[8] Lucas De Almeida and Geovanio Claudino Cavalcante Filho, "CFD Analysis of Drag Force for Different Nose Cone Design Potiguar Rocket Design View Project CFD Analysis of Drag Force for Different Nose Cone Design," Brasilia, Oct. 2019. [Online]. Available: https://www.researchgate.net/publication/336345689

[9] Emma Renee Fraley, "Design, Manufacturing, and Integration of Fins for 2017-2018 OSU ESRA 30k Rocket," Oregon, Oct. 2018.

[10] "ANSYS".

[11] G. Marra *et al.*, "A Wide Characterization of Aluminum Powders for Propellants A WIDE CHARACTERIZATION OF ALUMINUM POWDERS FOR PROPELLANTS *," 2004. [Online]. Available: https://www.researchgate.net/publication/280836428

[12] K. George, B. P. Panda, S. Mohanty, and S. K. Nayak, "Recent developments in elastomeric heat shielding materials for solid rocket motor casing application for future perspective," *Polymers for Advanced Technologies*, vol. 29, no. 1. John Wiley and Sons Ltd, pp. 8–21, Jan. 01, 2018. doi: 10.1002/pat.4101.

[13] R. Haymes and E. Gal, "Transient thermal multiscale analysis for rocket motor case: Mechanical homogenization approach," *Journal of Thermophysics and Heat Transfer*, vol. 31, no. 2, pp. 324–336, 2017, doi: 10.2514/1.T4929.

[14] E. S. Habib, M. A. El-Hadek, and A. El-Megharbel, "Stress analysis for cylinder made of FGM and subjected to thermo-mechanical loadings," *Metals (Basel)*, vol. 9, no. 1, Jan. 2019, doi: 10.3390/met9010004.

[15] K. Hu, F. Zhu, J. Chen, N. A. Noda, W. Han, and Y. Sano, "Simulation of thermal stress and fatigue life prediction of high speed steel work roll during hot rolling considering the initial residual stress," *Metals (Basel)*, vol. 9, no. 9, Sep. 2019, doi: 10.3390/met9090966.

[16] L. A. N. Wibawa, K. Diharjo, W. W. Raharjo, and B. H. Jihad, "Stress analysis of thick-walled cylinder for rocket motor case under internal pressure," *Journal of Advanced Research in Fluid Mechanics and Thermal Sciences*, vol. 70, no. 2, pp. 106–115, 2020, doi: 10.37934/ARFMTS.70.2.106115.

[17] M. Arefi and G. H. Rahimi, "Thermo elastic analysis of a functionally graded cylinder under internal pressure using first order shear deformation theory," *Scientific Research and Essays*, vol. 5, no. 12, pp. 1442–1454, 2010, [Online]. Available: http://www.academicjournals.org/SRE

[18] V. Vullo, "Springer Series in Solid and Structural Mechanics 3 Circular Cylinders and Pressure Vessels." [Online]. Available: http://www.springer.com/series/10616

[19] Z.-B. Shen, L. Zhang, and Y.-F. Li, "Structural integrity analysis and experimental investigation for solid rocket motor grain subjected to low temperature ignition," *MATEC Web of Conferences*, vol. 293, p. 04005, 2019, doi: 10.1051/matecconf/201929304005.